

EOS at FAIR energies and the role of resonances

E E Zabrodin^{†‡}, I C Arsene[†], J Bleibel[§], M Bleicher^{||},
 L V Bravina[†], G Burau^{||}, Amand Faessler[§], C Fuchs[§],
 M S Nilsson[†], K Tywoniuk[¶], H Stöcker^{|| + *}

[†] Department of Physics, University of Oslo, Oslo, Norway

[‡] Institute for Nuclear Physics, Moscow State University, Moscow, Russia

[§] Institute for Theoretical Physics, University of Tübingen, Tübingen, Germany

^{||} Institute for Theoretical Physics, University of Frankfurt, Frankfurt am Main, Germany

[¶] Departamento de Física de Partículas, Universidad de Santiago de Compostela, Santiago de Compostela, Spain

⁺ Gesellschaft für Schwerionenforschung mbH, Darmstadt, Germany

^{*} Frankfurt Institute for Advanced Studies (FIAS), University of Frankfurt, Frankfurt am Main, Germany

Abstract. Two microscopic models, UrQMD and QGSM, are used to extract the effective equation of state (EOS) of locally equilibrated nuclear matter produced in heavy-ion collisions at energies from 11.6 AGeV to 160 AGeV. Analysis is performed for the fixed central cubic cell of volume $V = 125 \text{ fm}^3$ and for the expanding cell that followed the growth of the central area with uniformly distributed energy. For all reactions the state of local equilibrium is nearly approached in both models after a certain relaxation period. The EOS has a simple linear dependence $P = c_s^2 \varepsilon$ with $0.12 \leq c_s^2 \leq 0.145$. Heavy resonances are shown to be responsible for deviations of the $c_s^2(T)$ and $c_s^2(\mu_B)$ from linear behavior. In the T - μ_B and T - μ_S planes the EOS has also almost linear dependence and demonstrates kinks related not to the deconfinement phase transition but to inelastic freeze-out in the system.

1. Introduction

One of the principle questions of the Compressed Baryon Matter (CBM) experiment at GSI FAIR is the equation of state of hot and dense matter produced in heavy-ion collisions at energies about 20 - 40 AGeV [1]. Because the perturbative quantum chromodynamics (pQCD) is not applicable to soft processes with small momentum transfer, one has to rely on microscopic models that correctly describe many features of the collisions at various energies. Two of such models, ultra-relativistic quantum molecular dynamics (UrQMD) [2] and quark-gluon string model (QGSM) [3], are used to extract the effective EOS of the excited matter in heavy-ion collisions at bombarding energies ranging from AGS to SPS. The UrQMD and, to a lesser extent, QGSM were already employed for studying the equilibration processes, see [4, 5]. Recently we modified the analysis by extending it to a non-fixed cell, which should follow the expanding area of uniformly distributed energy density [6]. By using both the UrQMD and QGSM for studies of the relaxation process in a broad energy range one can expect that the model-dependent effects, caused by application of a particular event generator, will be significantly reduced. - The models use different mechanisms

of string excitation and fragmentation. UrQMD relies on the longitudinal excitation, whereas the color exchange scheme is employed in QGSM. The fragmentation functions that determine the energy, momentum, and the type of the hadrons produced during the string decay are also different. Finally, both models do not use the same tables of hadrons, chosen as discrete degrees of freedom. Whereas the UrQMD contains 55 baryon and 32 meson states together with their antistates, the QGSM takes into account octet and decuplet baryons, and nonets of vector and pseudoscalar mesons, as well as their antiparticles. Heavy resonances are not included in the current version of the QGSM, and this circumstance can be used to elaborate on their role in the EOS.

Central gold-gold collisions with zero impact parameter $b = 0$ fm were simulated at bombarding energies $E_{\text{lab}} = 11.6, 20, 30, 40, 80$ and 160 AGeV, respectively. The total energy, the net baryon charge and the net strangeness extracted for a certain volume of the reaction, were inserted into a system of nonlinear equations [4] to obtain temperature T , baryon chemical potential μ_B and strangeness chemical potential μ_S of an ideal hadron gas in equilibrium. If the yields and transverse momentum spectra of particles obtained in a snapshot of microscopic simulations at time t were close to the results of statistical model (SM), the matter in the cell is considered to be in the vicinity of equilibrium. Then its equation of state can be derived and studied. Because the cell is an open system with instantly changing energy and particle density, the verification of the equilibrium conditions is repeated after a time-step of $\Delta t = 1$ fm/c.

2. Relaxation to equilibrium and EOS in the cell.

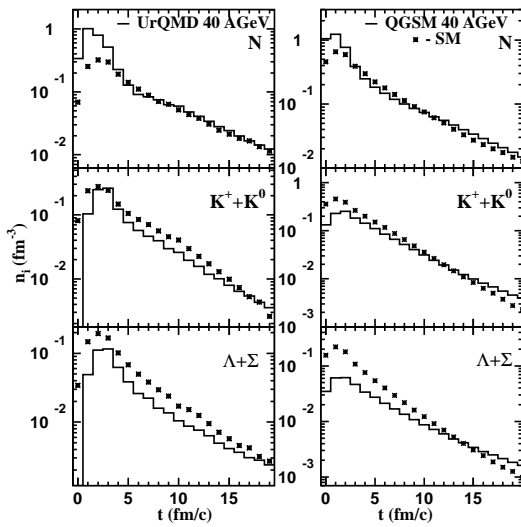


Figure 1. Hadron yields in the central $V = 125 \text{ fm}^3$ cell of central Au+Au collisions at 40 AGeV in microscopic models (histograms) and statistical model (symbols).

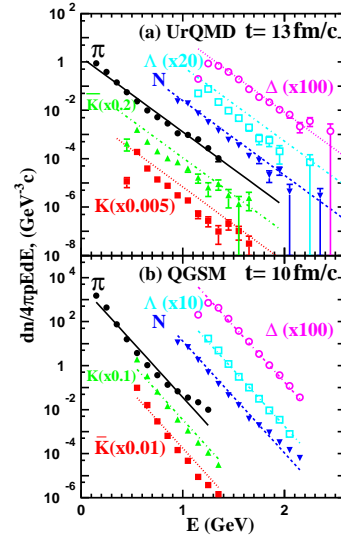


Figure 2. Energy spectra of hadrons in the central $V = 125 \text{ fm}^3$ cell.

In the standard approach the test-volume was a fixed central cubic cell of $V = 125 \text{ fm}^3$. The yields of some hadron species are displayed in Fig. 1 for central gold-

gold collisions at $E_{\text{lab}} = 40$ AGeV. The agreement between the results of microscopic and statistical model calculations is good after $t \geq 9$ fm/c. Here the standard criterion $[yield(mic) - yield(SM)]/error(SM) \leq 1$ is applied. According to model analysis, after $t \approx 10$ fm/c almost all many-body processes going via the formation of strings or many-particle decaying resonances are ceased, and one deals mainly with elastic and quasi-elastic reactions. The energy spectra $dN/4\pi p E dE$ calculated microscopically are shown in Fig. 2. The Boltzmann fit to particle distributions is presented in Fig. 2 as well. Both in UrQMD and in QGSM the energy spectra agree well with the exponential form of the Boltzmann distributions. Because the hadronic matter in the central cell nearly reaches the state of thermal and chemical equilibrium, the macroscopic thermodynamic parameters of the system, such as temperature and chemical potentials, become meaningful.

Isentropic expansion of relativistic fluid is one of the main postulates of Landau hydrodynamic theory [7] of multiparticle production. As can be seen in Fig. 3 the entropy per baryon ratio is nearly conserved in the equilibrium phase of the expansion within the 5% accuracy limit. The entropy densities s obtained for the cell in both models are very close to each other, but, because of the difference in net-baryon sector, the ratio s/ρ_B in UrQMD is about 15–20% larger than that in QGSM.

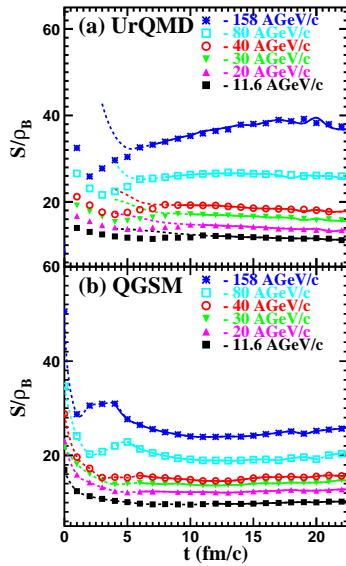


Figure 3. Entropy per baryon in the central cell as a function of time t .

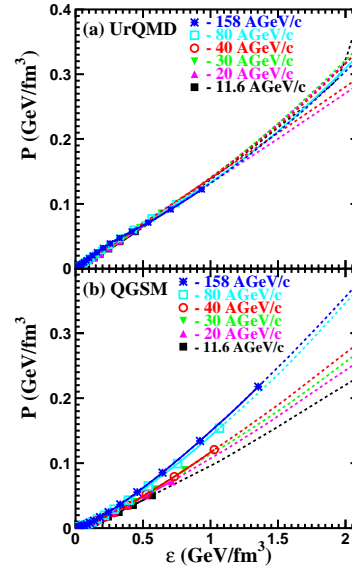


Figure 4. Equation of state: microscopic pressure P vs. the energy density ε .

Any hydrodynamic model relies on the equation of state, which links the pressure of the system to its energy density. Otherwise, the system of hydrodynamic equations is incomplete. The corresponding plot with microscopic pressures $P_{\text{mic}}(\varepsilon)$ is presented in Fig. 4. For both models the shapes of the distributions are very close to linear for all energies in question. Thus the EOS has a rather simple form

$$P(\varepsilon) = c_s^2 \varepsilon, \quad (1)$$

where the sonic velocity in the medium $c_s = (dP/d\varepsilon)^{1/2}$ is fully determined by the slopes of the distributions $P(\varepsilon)$. To account for possible deviations from a straight line

behavior the slopes of the functions P versus ε were averaged over the whole period of the equilibrated phase. For the UrQMD calculations the velocity of sound increases from 0.13 at $E_{\text{lab}} = 11.6$ AGeV to 0.146 at $E_{\text{lab}} = 158$ AGeV. It saturates at $c_s^2 \approx 0.15$ for RHIC energies [4]. That corresponds to change of the nuclear compressibility from 140 MeV (AGS) to 200 MeV (SPS and RHIC). In QGSM calculations the averaged sound velocity is about 0.015 units smaller. Note that due to the averaging over time, respectively energy density, these values are lower the maximal values for c_s^2 that are reached in the corresponding reactions. Both models indicate that at the energy around $E_{\text{lab}} = 40$ AGeV the slope of the $c_s^2(\sqrt{s})$ distribution is changing, and the velocity of sound becomes less sensitive to rising bombarding energy.

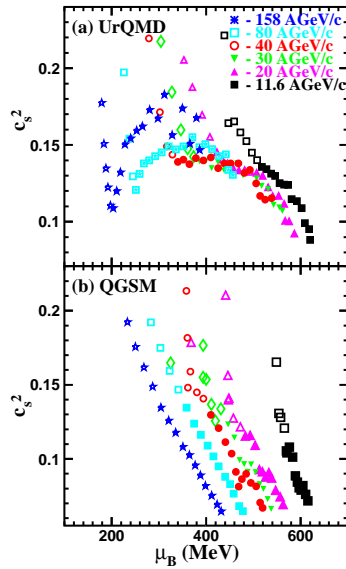


Figure 5. The sound velocity c_s^2 in the central cell of volume $V = 125 \text{ fm}^3$ as a function of baryon chemical potential μ_B .

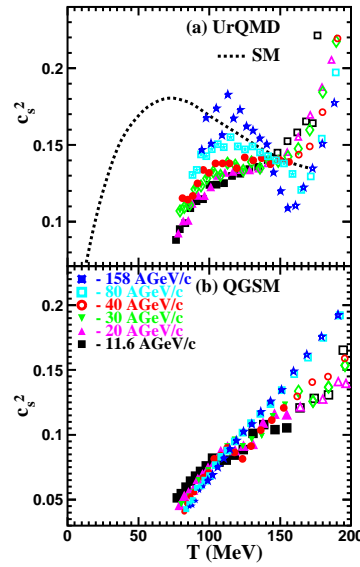


Figure 6. Temperature dependence of the sound velocity. Dashed line corresponds to calculations within Hagedorn model of ideal hadron gas.

Figure 5 shows the dependence of the c_s^2 on the baryon chemical potential μ_B . For three bombarding energies, $E_{\text{lab}} = 20$ AGeV, 30 AGeV, and 40 AGeV, the functions $c_s^2(\mu_B)$ are close to each other. In QGSM calculations c_s^2 depends linearly on μ_B and the slope c_s^2/μ_B is unique for all reactions. In UrQMD the picture is more complex. For the late stages of system evolution the slopes of all distributions are also similar, but for energies of $E_{\text{lab}} \geq 40$ AGeV one sees the rise of the sound velocity at the beginning of the equilibration, plateau, and the falloff. This can be taken as indication of the role of heavy resonances, because their fraction is presented in the particle spectrum at the early period and disappeared completely at the end. These resonances are rare at $E_{\text{lab}} \leq 20$ AGeV, and distributions $c_s^2(\mu_B)$ obtained in both models are quite similar.

The obtained EOS is soft, because for the ultrarelativistic gas of light particles the sonic speed is $c_s = 1/\sqrt{3}$. But the presence of resonances in particle spectrum generates the decrease [8] of the c_s . Employing the empirical dependence $\rho(m) \propto m^{\alpha'}$, $2 \leq \alpha' \leq 3$ [9], where $\rho(m) dm$ denotes the number of resonances with masses

from m to $m + dm$, one arrives to the equation of state in the form [8]

$$\varepsilon = (\alpha' + 4) P , \quad (2)$$

i.e., $\frac{1}{7} \leq c_s^2 \leq \frac{1}{6}$. This result is reproduced in microscopic models. Note that PHENIX collaboration reported the value $c_s \approx 0.35 \pm 0.05$ [11], i.e., $c_s^2 \approx 0.12 \pm 0.3$, for Au+Au collisions at top RHIC energy $\sqrt{s} = 200$ AGeV. This value is close to our results and also implies rather soft effective EOS.

Temperature dependence of the sonic speed $c_s^2(T)$ is depicted in Fig. 6 together with the EOS calculated in [10] within the Hagedorn model with $\mu = 0$. For $E_{\text{lab}} = 80$ AGeV and 160 AGeV the UrQMD data exhibit a falloff in $c_s^2(T)$ at $T \geq 120$ MeV in accord with the Hagedorn model. This decrease is assigned to heavy resonances, because neither the UrQMD calculations at lower energies nor the QGSM calculations without the heavy resonances reveal the negative slope in the equation of state $c_s^2(T)$. Below $T = 100$ MeV both microscopic models indicate rapid drop of the sound velocity that occurs much earlier compared to that of the Hagedorn model.

In the modified analysis the central cell was further subdivided into the smaller ones embedded one into another. If the ε of the inner cell is not the same (within the 5% limit of accuracy) as the energy density of the outer one, the SM analysis of the thermodynamic conditions is performed for the inner cell, otherwise the outer cell becomes a new test volume. This permits one to follow the expansion of the area with uniformly distributed energy. EOS in the $T - \mu_B$ plane is shown in Fig. 7. Symbols and dashed lines show the evolution of these quantities in a cell of instantly increasing volume ($V_{\text{init}} = 0.125 \text{ fm}^3$), whereas dotted (upper plot) and full (both plots) lines are related to calculations with the fixed volume $V = 125 \text{ fm}^3$. The transition to equilibrium proceeds quite smoothly if the analysis is performed for the fixed cell. In contrast, in the area with uniformly distributed energy the transition is characterized by a kink distinctly seen in each of the phase diagrams in both microscopic models. The effect, which takes place along the lines of the constant entropy per baryon, is caused by the significant reduction of the number of processes going via the formation and fragmentation of strings, i.e., chemical freeze-out. The observed phenomenon can easily mimic the signature of the QCD phase transition in the $T - \mu_B$ plane. Evolution of strangeness chemical potential μ_S with T in the fixed volume and non-fixed volume is displayed in Fig. 8. As in Fig. 7, all systems develop kinks in the $T(\mu_S)$ distributions precisely at the moment of transition from nonequilibrium to equilibrium phase. Both baryon density and strangeness density are decreasing in the test volume, however, the baryon chemical potential increases with time, whereas the strangeness one drops. The evolution of the μ_S and μ_B with T proceeds quasilinearly, thus reducing the deviations, caused by nonzero chemical potentials, of the functions $\varepsilon(T)$ and $s(T)$ from the ideal gas behavior at $\mu = 0$.

3. Conclusions

In summary, both microscopic models favor the formation of the equilibrated matter for a period of about $10 \text{ fm}/c$ for all reactions in question. During this period the matter in the central cell expands with constant entropy per baryon. The equation of state can be approximated by a simple linear dependence $P = a(\sqrt{s})\varepsilon$, where the square of the speed of sound $c_s^2 = a(\sqrt{s})$ varies from 0.13 (AGS) to 0.15 (SPS) in the UrQMD calculations and from 0.11 (AGS) to 0.14 (SPS) in the QGSM ones.

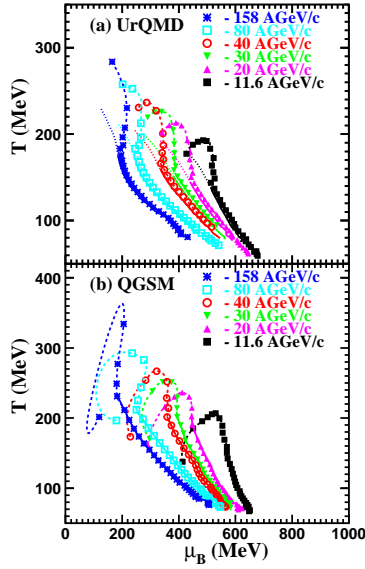


Figure 7. Temperature T vs. baryon chemical potential μ_B .

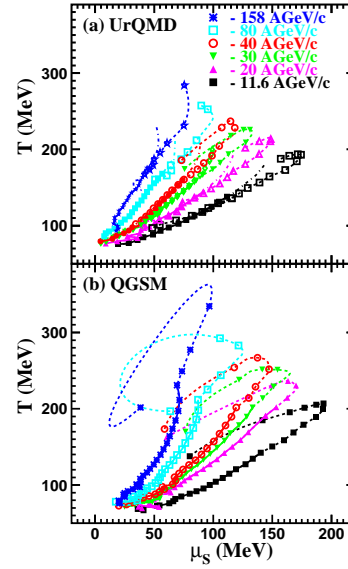


Figure 8. Temperature T vs. strangeness chemical potential μ_S .

Heavy resonances are responsible for negative slope in $c_s^2(T)$ at $T \geq 100$ MeV in accord with the predictions of Hagedorn model of hadron resonance gas. At lower temperatures both microscopic models indicate a rapid drop of the sonic speed in stark contrast with the Hagedorn model calculations with zero chemical potential.

Study of the expanding area of isotropically distributed energy reveals that the relaxation to equilibrium in this dynamic region proceeds at the same rate as in the case of the fixed-size cell. However, here both microscopic models unambiguously show the presence of a kink in the T - μ_B phase diagrams. The higher the collision energy, the earlier the kink formation. Its origin is linked to the freeze-out of inelastic reactions in the considered area.

Acknowledgments. This work was supported by the Norwegian Research Council (NFR) under contract no. 185664/V30, by the DFG and the BMBF.

References

- [1] Henning W F 2007 *J. Phys. G: Nucl. Phys.* **34** S551
- [2] Bass S A et al 1998 *Prog. Part. Nucl. Phys.* **41** 255
- [3] Bleicher M et al 1999 *J. Phys. G: Nucl. Phys.* **25** 1859
- [4] Amelin N S, Bravina L V 1990 *Sov. J. Nucl. Phys.* **51** 133
Amelin N S et al 1993 *Phys. Rev.* **C47** 2299
- [5] Bravina L V et al 1998 *Phys. Lett.* **B434** 379
Bravina L V et al 1999 *Phys. Rev.* **C60** 024904
Bravina L V et al 2001 *Phys. Rev.* **C63** 064902
- [6] Bleibel J et al 2006 *Nucl. Phys.* **A767** 218
- [7] Bravina L V et al 2008 *Phys. Rev.* **C78** 014907
- [8] Landau L D 1953 *Izv. Akad. Nauk SSSR, Ser. Fiz.* **17** 51
- [9] Shuryak E 1973 *Sov. J. Nucl. Phys.* **16** 220
- [10] Hagedorn R 1965 *Nuovo Cimento Suppl.* **3** 147
- [11] Chojnacki M, Florkowski W, Csörgö T 2005 *Phys. Rev.* **C71** 044902
- [12] PHENIX Collaboration, A. Adare et al 2007 *Phys. Rev. Lett.* **98** 162301